BBA - Molecular and Cell Biology of Lipids 1868 (2023) 159377

Contents lists available at ScienceDirect

BBA - Molecular and Cell Biology of Lipids

journal homepage: www.elsevier.com/locate/bbalip

Functionally diverse front-end desaturases are widespread in the phylum Annelida

Marc Ramos-Llorens [a], Francisco Hontoria [a], Juan C. Navarro [a], David E.K. Ferrier [b], Óscar Monroig [a,*]

[a] Instituto de Acuicultura Torre de la Sal (IATS), CSIC, 12595 Ribera de Cabanes, Castellón, Spain
[b] The Scottish Oceans Institute, School of Biology, University of St. Andrews, St Andrews, Fife KY16 8LB, UK

ARTICLE INFO

Keywords:
Annelida
Biosynthesis
Front-end desaturases
Functional diversity
Long-chain polyunsaturated fatty acids

ABSTRACT

Aquatic single-cell organisms have long been believed to be unique primary producers of omega-3 long-chain ($\geq C_{20}$) polyunsaturated fatty acids (ω3 LC-PUFA). Multiple invertebrates including annelids have been discovered to possess methyl-end desaturases enabling key steps in the de novo synthesis of ω3 LC-PUFA, and thus potentially contributing to their production in the ocean. Along methyl-end desaturases, the repertoire and function of further LC-PUFA biosynthesising enzymes is largely missing in Annelida. In this study we examined the front-end desaturase gene repertoire across the phylum Annelida, from Polychaeta and Clitellata, major classes of annelids comprising most annelid diversity. We further characterised the functions of the encoded enzymes in selected representative species by using a heterologous expression system based in yeast, demonstrating that functions of Annelida front-end desaturases have highly diversified during their expansion in both terrestrial and aquatic ecosystems. We concluded that annelids possess at least two front-end desaturases with Δ5 and Δ6Δ8 desaturase regioselectivities, enabling all the desaturation reactions required to convert the C_{18} precursors into the physiologically relevant LC-PUFA such as eicosapentaenoic and arachidonic acids, but not docosahexaenoic acid. Such a gene complement is conserved across the different taxonomic groups within Annelida.

1. Introduction

Long-chain ($\geq C_{20}$) polyunsaturated fatty acids (LC-PUFA) are essential biomolecules that play key roles in cell structure, metabolism, lipid signalling and gene regulation of both aquatic and terrestrial animals [1–3]. LC-PUFA with well-demonstrated functions in the above biological processes include the "omega-6" (ω6 or n-6) LC-PUFA arachidonic acid (ARA, 20:4n-6), and the "omega-3" (ω3 or n-3) eicosapentaenoic (EPA, 20:5n-3) and docosahexaenoic (DHA, 22:6n-3) acids. Importantly, ω3 LC-PUFA have been associated with health benefits in a variety of conditions that affect humans [4–7], and with an increasing prevalence of such pathologies, there is an interest in understanding the production of ω3 LC-PUFA at a global scale [8,9]. Virtually all the production of ω3 LC-PUFA occurs in the ocean; in contrast, terrestrial and freshwater aquatic ecosystems are comparatively poor in ω3 LC-PUFA and are instead regarded as sources of short-chain metabolic precursors [2,3]. Primary production of ω3 LC-PUFA in marine ecosystems has been associated almost exclusively with the activity of single-cell organisms, including microalgae, heterotrophic protists and bacteria [10]. Yet, this long-standing paradigm has recently been challenged by the discovery that multiple invertebrates, including cnidarians, nematodes, rotifers, molluscs, arthropods and annelids, possess LC-PUFA biosynthesising enzymes termed "methyl-end" (or "ω") desaturases that, like in aquatic microbes, enable the de novo biosynthesis of ω3 LC-PUFA [11]. Attempts to quantify the production of ω3 LC-PUFA by marine phytoplankton have been made [8] and predictive models point towards a decline of ω3 LC-PUFA produced by marine microbes as a consequence of the increasing seawater temperature [9]. The contribution of invertebrates to global ω3 LC-PUFA production cannot yet be estimated due to, among other reasons, the lack of accurate quantification of biomass abundance, which is particularly challenging in groups inhabiting aquatic ecosystems. However, it is important to shed light on the capacity that certain groups of invertebrates have to endogenously produce ω3 LC-PUFA that can be

* Corresponding author at: Instituto de Acuicultura Torre de la Sal (IATS, CSIC), Consejo Superior de Investigaciones Científicas, 12595 Ribera de Cabanes, Castellón, Spain.
E-mail address: oscar.monroig@csic.es (Ó. Monroig).

https://doi.org/10.1016/j.bbalip.2023.159377
Received 2 June 2023; Received in revised form 24 July 2023; Accepted 27 July 2023
Available online 29 July 2023

transferred to upper-level consumers including fish, and thus partly alleviate the deleterious consequence of limiting the supply of physiologically important nutrients alluded to above [12].

A key step in establishing the capacity of invertebrates for ω3 LC-PUFA production requires an understanding of the repertoire of genes and functions involved in their biosynthetic pathways (Fig. 1) [13]. All living organisms possess the enzymatic capacity for biosynthesising saturated fatty acids (FA) such as palmitic acid (16:0) and stearic acid (18:0) and, from them, monounsaturated FA through the action of "first" desaturases with Δ9 desaturase activity [13]. Importantly, while the above enzymatic capacities are widespread in animals, the introduction of further double bonds enabling the de novo biosynthesis of polyunsaturated fatty acids (PUFA) is absent in vertebrates. As noted above, multiple species within cnidarians, nematodes, rotifers, molluscs, arthropods and annelids have methyl-end desaturase enzymes enabling them to synthesise PUFA, including linoleic acid (LA, 18:2n-6) and α-linoleic acid (ALA, 18:3n-3). While they do not play biologically relevant roles themselves, both LA and ALA are precursors of the ω6 and ω3 LC-PUFA, respectively, via the action of two enzyme types, namely elongation of very long-chain fatty acid (Elovl) proteins and front-end desaturases. The repertoire of Elovl and front-end desaturases that mediate the biosynthesis of LC-PUFA from C_{18} PUFA precursors (LA and ALA) varies among species [13]. It is widely accepted that the LC-PUFA biosynthesising capacity in animals is often limited at the desaturase level due to their rather strict substrate specificity compared to Elovl enzymes [14]. Hence, an extensive characterisation of the desaturase complements within a given invertebrate phylum provides a good understanding of the capacity for the biosynthesis of LC-PUFA of its representative groups.

Previous studies have demonstrated that polychaetes (Annelida), including the deep-sea giant tubeworm *Riftia pachyptila* [15], and the nereids *Platynereis dumerilii* [11] and *Hediste diversicolor* [16], possess methyl-end desaturases. However, to the best of our knowledge, no front-end desaturases have yet been characterised in Annelida, although early studies provided evidence suggesting that some polychaetes have shown desaturation capacity consistent with the presence of this enzyme type [17–19]. Surprisingly, despite the remarkable diversity of the phylum Annelida and the importance of members of this group for nutrient recycling in both terrestrial and aquatic ecosystems, a comprehensive investigation of the front-end desaturase family in Annelida is lacking. The present study aimed to provide a comprehensive overview of the occurrence of front-end desaturase encoding genes in representative species from Polychaeta and Clitellata, major classes of annelids comprising most annelid diversity [20]. Along with the examination of the front-end desaturase gene repertoire across the phylum Annelida, we further characterised the functions of the encoded enzymes in selected representative species by using a heterologous expression system based in yeast, demonstrating that functions of Annelida front-end desaturases have highly diversified during their expansion in both terrestrial and aquatic ecosystems.

2. Materials and methods

2.1. Gene identification and sequence analysis of annelid front-end desaturases

To identify putative sequences of front-end desaturases within Annelida, sequence retrieval was performed through Basic Local Alignment Search Tool (BLAST) (https://blast.ncbi.nlm.nih.gov/Blast.cgi) against Transcriptome Shotgun Assembly (TSA) databases from Annelid organisms [Annelida (taxid: 6340)] using the sequences of front-end desaturases characterised from *Octopus vulgaris* (AEK20864; [21]) and *Danio rerio* (AF309556; [22]) as queries. Putative full-length open reading frames (ORF) were predicted using Open Reading Frame Finder (ORFfinder) (https://www.ncbi.nlm.nih.gov/orffinder). Protein identification and classification were confirmed using the prediction

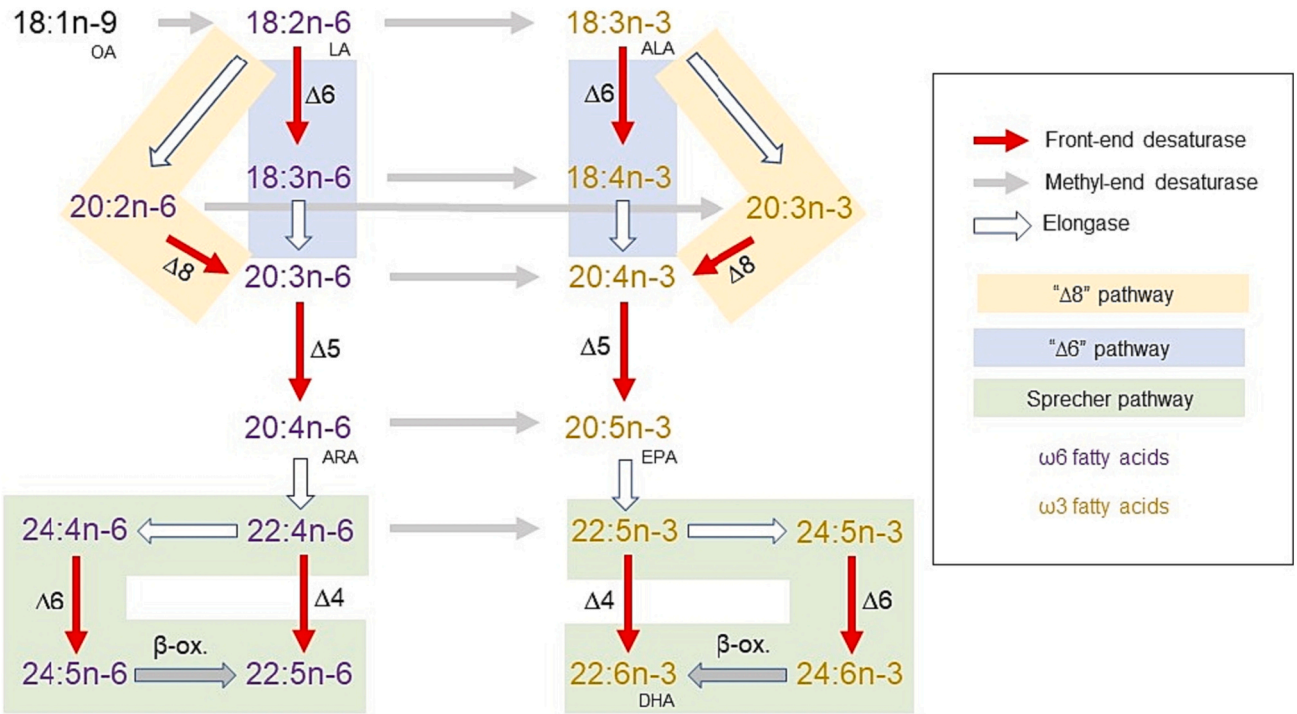

Fig. 1. The LC-PUFA biosynthetic pathways in animals (adapted from Monroig and Kabeya, 2018). Red arrows represent the reactions catalysed by front-end desaturases that are studied in this work, which include Δ4, Δ5, Δ6 or Δ8 desaturations. The initials below compound nomenclatures indicate the name of the most relevant fatty acids in the pathway including oleic acid (OA, 18:1n-9), linoleic acid (LA, 18:2n-6), α-linolenic acid (ALA, 18:3n-3), arachidonic acid (ARA, 20:4n-6), eicosapentaenoic acid (EPA, 20:5n-3) and docosahexaenoic acid (DHA, 22:6n-3). To simplify the diagram, reactions producing non-methylene-interrupted fatty acids are not included.

tool [23] from the Pfam database [24] (protein domains: *Cyt-b5* PF00173 and *FA_desaturase* PF00487) and InterProScan tool [25] from the InterPro database [26] (protein family membership: *Fatty acid desaturase* (IPR012171)). For sequences retrieved directly from genomes, exons were identified in chromosomes using BLAST against whole shot-gun genome projects, and then assembled by comparing against reference sequences using Geneious Prime Software (v: 2022.1.1; Biomatters, Inc., San Diego, USA). Further retrieval of the sequences was carried out by confirming the presence of diagnostic residues along the three conserved histidine (H) boxes that distinguish front-end desaturases from other desaturase types [27]. The alignment of retrieved putative protein sequences was carried out using MUSCLE [28].

2.2. Phylogenetic analysis of annelid front-end desaturase sequences

A phylogenetic tree comparing the deduced amino acid (aa) sequences of annelid desaturases with homologues retrieved from a variety of animals was constructed using the maximum-likelihood (ML) method. The phylogenetic analysis was performed using the user-customised workflow platform of the NGPhylogeny.fr server [29]. Representatives for all different subtypes of desaturase, namely methyl-end desaturases, front-end desaturases and "first" desaturases [27], were selected from different model species within relevant animal groups [13]. For invertebrates, desaturase sequences were selected from annelids with existing publicly accessible 'omic data', such as *Capitella teleta*, *Dimorphilus gyrociliatus*, *Eisenia fetida*, *Hirudo medicinalis*, *Lamellibrachia satsuma*, *Owenia fusiformis*, *Platynereis dumerilii*, *Sipunculus nudus*, *Spirobranchus lamarcki* and *Urechis unicinctus* [30–39]. In addition, species from other invertebrate groups, including crustaceans (e.g., *Tigriopus californicus* and *Platychelipus littoralis*) and molluscs (e.g., *O. vulgaris*) from which front-end desaturase enzymes have been previously characterised were included in the analysis [21,40]. Selected aa sequences were aligned with MAFFT [41]. The resulting alignment was trimmed with trimAl [42] before generating a ML phylogenetic tree using PhyML [43], and an automated model selection implemented in PhyML based on heuristic strategies with the SMS software [44]. The percentage of replicate trees and confidence in the resulting phylogenetic tree branch topology in which the associated taxa clustered together in the bootstrap test (1000 replicates) are shown next to the branches [45]. The resulting tree was processed in Newick format [46] and visualised using MEGA11 [47].

2.3. Sample collection, RNA extraction and cDNA synthesis

Phylogenetic analyses enabled the identification of a number of front-end desaturase subgroups within annelids that were represented by *P. dumerilii*, *E. fetida*, *S. lamarcki* (previously *Pomatoceros lamarcki*), *L. satsuma* and *U. unicinctus*. Further functional characterisation assays were performed on a selection of front-end desaturases from these species as detailed below. *P. dumerilii* individuals were kindly donated by Dr. Florian Raible from an established culture of the inbreed strain "PIN" [48] at the Max Perutz Labs Vienna (Vienna, Austria). *E. fetida* was purchased from a local composting supplier (Vermiorganic, Vejer de la Frontera, Spain). *S. lamarcki* were collected from the rockpools at East Sands, St Andrews, UK (56.33°N, 2.78°W) in 2015 and kept in the flow-through seawater system in the Scottish Oceans Institute, University of St Andrews, at close to ambient temperature until needed. Adult worms were removed from their calcified tubes by breaking the tubes open at the posterior end and then pushing the worms out from the anterior end with a blunt probe. After rinsing the worms in filtered seawater, they were transferred to RNAlater (Ambion) and kept in a fridge for a short time prior they were stored at −80 °C. Due to the unavailability of fresh samples from *L. satsuma* and *U. unicinctus*, the corresponding full-length ORF sequences (one sole sequence per species) were ordered as synthetic genes (Genscript Biotech, Leiden, The Netherlands). Total RNA extraction was carried out on *P. dumerilii*, *E. fetida* and *S. lamarcki* individual samples (~10 mg from the head region of one specimen) by homogenisation with a tissue disrupter in 1 ml of TRI reagent (Sigma-Aldrich) following the manufacturer's instructions (Thermo Fisher Scientific, Waltham, MA, USA). Next, 2 μg of total RNA were reverse transcribed into cDNA using Moloney Murine Leukaemia Virus Reverse Transcriptase (Promega, Madison, WI, USA) primed with random primers and oligo-dT primers (3:1 mol) (Promega). The cDNA was stored at −20 °C until further use. To verify the species identity for samples from putative *P. dumerilii*, *E. fetida* and *S. lamarcki*, a diagnostic 710 bp fragment of mitochondrial cytochrome *c* oxidase subunit I gene (COI) was amplified with specific DNA primers to identify invertebrates according to Folmer et al. [49]. The PCR product was purified using Wizard ® SV gel and PCR clean-up system purification kit (Promega) and further sequenced (DNA Sequencing Unit, IBMCP-CSIC-UPV, Valencia, Spain) to confirm the species identity.

2.4. Molecular cloning of full-length ORF from annelid front-end desaturases

Full-length ORF sequences of the front-end desaturases from *P. dumerilii* (3 sequences), *E. fetida* (3) and *S. lamarcki* (1) were amplified using the high-fidelity Phusion® DNA polymerase (Thermo Fisher Scientific). Primer pairs used to amplify the ORF sequences contained different restriction enzyme sites to enable further ligation into the yeast expression vector pYES2 (Thermo Fisher Scientific) used in the functional assays (Table 1). The PCR conditions were as follows: initial denaturing at 98 °C for 3 min, 40 cycles of denaturation at 98 °C for 30 s, annealing at 55 °C for 30 s, extension at 72 °C for 45 s, and a final extension at 72 °C for 10 min. PCR products were separated through electrophoresis in 1 % (w/v) agarose gel and subsequently purified with Wizard ® SV Gel and PCR Clean-Up System (Promega) purification kit. Double digestions with the corresponding restriction enzymes (Table 1) were carried out with CutSmart® Buffer (New England Biolabs, Ipswich, MA, USA) at 37 °C according to the manufacturer's instructions. The restricted PCR products were purified as above and subsequently ligated into a similarly restricted yeast expression vector pYES2 using T4 DNA ligase (Promega). Synthetic ORF sequences from *L. satsuma* and *U. unicinctus*, originally cloned into pUC57 (Genscript Biotech), were subcloned into pYES2 as indicated above. Collectively, a total of nine ORF front-end desaturase sequences were cloned into pYES2, resulting in three constructs for *P. dumerilli* (pYES2-PDfed1, pYES2-PDfed2, pYES2-PDfed3), three for *E. fetida* (pYES2-EFfed1, pYES2-EFfed2, pYES2-EFfed3), one for *S. lamarcki* (pYES2-SLfed), one for *L. satsuma* (pYES2-LSfed), and one for *U. unicinctus* (pYES2-UUfed). Preparation of the pYES2 constructs was carried out as detailed by Kabeya et al. [40]. Briefly, ligation reactions (T4 ligase, Promega) of each ORF sequence

Table 1
List of primers used for molecular cloning. Restriction enzymes used for cloning into the yeast expression vector pYES2 are named at the end of the primer name. Restriction sites in primer sequences are underlined.

Primer name	Sequence 5′-3′
PD-fed1-For-*Hin*dIII	CCCAAGCTTAAGATGGGGAAAGGC
PD-fed1-Rev-*Xba*I	GCTCTAGATCCTCAGTGTGAATCCATGTG
PD-fed2-For-HindIII	CCCAAGCTTACCATGGGAAAAGGTGC
PD-fed2-Rev-XbaI	GCTCTAGATCATCATTGATGGTGGTAGGC
PD-fed3-For-HindIII	CCCAAGCTTATGGGGAAAGGAC
PD-fed3-Rev-*Xho*I	GCCTCGAGGTATTCATGTATGGT
SL-fed1-For-HindIII	CCCAAGCTTGGGATGGGCAAAGGCG
SL-fed1-Rev-XhoI	CCGCTCGAGCGGTTACTGGAGATGAT
EF-fed1-For-BamHI	CGGGATCCCGATGGGTAAGGGTG
EF-fed1-Rev-XbaI	GCTCTAGAGCTTATGATACATGGTACGACTG
EF-fed2-For-*Sac*I	CGAGCTCGATGAACGGGAAGACC
EF-fed2-Rev-XbaI	GCTCTAGAGCTCAGGAATTCAGTTTCTTG
EF-fed3-For-BamHI	CGGGATCCCGATGGGCAAAGG
EF-fed3-Rev-XbaI	GCTCTAGAGCCTAACCGTTATATGCGTC

into similarly rescripted pYES2 were transformed into *E. coli* Top10' competent cells and grown in Luria-Bertani (LB) agar plates with ampicillin (100 μg ml^{-1}) for selection of positive colonies. Subsequently, colonies were screened by PCR and grown overnight in LB broth with ampicillin (100 μg ml^{-1}). Overnight cultures were processed for plasmid preparation (GenElute™ Plasmid Miniprep Kit, Sigma-Aldrich). Correctness of the ORF sequences was confirmed by Sanger DNA sequencing (DNA Sequencing Unit, IBMCP-UPV, Valencia, Spain) prior to use in the functional characterisation assays in yeast.

2.5. Functional characterisation by heterologous expression in yeast

Plasmid constructs containing the ORF of selected front-end desaturases (pYES2-PDfed1, pYES2-PDfed2, pYES2-PDfed3, pYES2-EFfed1, pYES2-EFfed2, pYES2-EFfed3, pYES2-SLfed, pYES2-LSfed and pYES2-UUfed) were transformed into competent *Saccharomyces cerevisiae* INv*Sc*1 cells (Thermo Fisher Scientific) using the *S.c.* EasyComp® Transformation kit (Thermo Fisher Scientific). Transformed yeast were cultured on *S. c.* minimal medium minus uracil ($SCMM^{-ura}$) agar plates at 30 °C for 3 d. Subsequently, one single colony from each plate was grown in $SCMM^{-ura}$ broth at 30 °C for 2 d until reaching an OD_{600} between 8 and 10. Next, subcultures of 5 ml with a starting cell density of $OD_{600} = 0.4$ were set in each of the 150 ml Erlenmeyer flasks used to test each of the eight desaturase PUFA substrates assayed. After 4 h of constant shaking at 30 °C, transgenic yeast cultures were supplemented with galactose (2 %, w/v) to induce gene expression, as well as an aliquot of a PUFA substrate. A total of eight substrates for front-end desaturases, selected according to the currently accepted animal LC-PUFA biosynthetic pathways (Fig. 1) [13,50] were assayed: linoleic acid (LA, 18:2n-6) and α-linolenic acid (ALA, 18:3n-3) as Δ6 desaturase substrates, eicosadienoic acid (20:2n-6) and eicosatrienoic acid (20:3n-3) as Δ8 desaturase substrates, dihomo-γ-linoleic acid (20:3n-6) and eicosatetraenoic acid (20:4n-3) as Δ5 desaturase substrates, and docosatetranoic acid (22:4n-6) and docosapentanoic acid (22:5n-3) as Δ4 desaturase substrates. Moreover, transgenic yeast expressing the Δ6 front-end desaturase from *U. unicinctus* (UUfed, OQ102611) were grown in the presence of 24:5n-3, to test its ability to contribute to the DHA synthesis via the Sprecher Pathway (Sprecher, 2000) (Fig. 1). Each PUFA substrate was supplemented as sodium salts at concentrations of 0.5 mM (C_{18}), 0.75 mM (C_{20}), 1.0 mM (C_{22}) and 1.25 mM (C_{24}) to compensate for the reduced uptake efficiency with the length of the carbon chain. The yeast cultures were maintained at 30 °C and under constant shaking (250 rpm) for 2 d until yeast was harvested by centrifugation at 1500*g* for 2 min. Yeast pellets were washed twice with 5 ml of ddH_2O, homogenised in 6 ml of 2:1 (*v*/v) chloroform:methanol containing 0.01 % (w/v) butylated hydroxytoluene (BHT, Sigma-Aldrich) as an antioxidant, and stored at −20 °C for a minimum of 24 h in an oxygen-free atmosphere until further analysis.

2.6. Fatty acid analysis

Total lipids were extracted from the homogenised yeast samples using Folch's method [51] with modifications as described by Ribes-Navarro et al. [52]. Fatty acid methyl esters (FAME) from the total lipids were prepared by acid catalysed methylation for 16 h at 50 °C [53]. FAME were subsequently purified by thin-layer chromatography and analysed on a gas chromatograph (GC) (Thermo Trace GC Ultra, Thermo Electron Corporation, Waltham, MA, USA) fitted with an on-column injection system, a flame ionisation detector (FID), and a silica capillary column (30 m × 0.25 mm × 0.25 μm film thickness, TR-WAX, Teknokroma, Spain), using helium as a carrier gas. The proportion of each PUFA substrate converted to the corresponding desaturated product was calculated as [product area / (product area + substrate area)] × 100.

3. Results

3.1. Sequences and phylogeny of annelid front-end desaturases

Front-end desaturase candidates from annelids were identified in Clitellata and Polychaeta representative species including *C. teleta*, *D. gyrociliatus*, *E. fetida*, *H. medicinalis*, *L. satsuma*, *O. fusiformis*, *P. dumerilii*, *S. nudus*, *S. lamarcki* and *U. unicinctus* (Tables S1; S2). The deduced aa sequences of all the annelid front-end desaturases retrieved through our search strategy contained all characteristic front-end desaturase conserved motifs, including a heme-binding motif (HPGG), and three H boxes (HXXXH, HXXHH and QXXHH) (Fig. S1). Furthermore, the third conserved H box starts in the identified candidate sequences with a glutamine (Q) residue as expected for front-end desaturases according to the motifs described by Hashimoto et al. [27].

The ML phylogenetic subtree built with the selected front-end desaturases is shown in Fig. 2 (the complete ML phylogenetic tree is shown in Fig. S2). All the annelid front-end desaturases were contained within two main clades identified as group A and group B (Fig. 2) according to the nomenclature of front-end desaturase groups proposed by Surm et al. [54,55] for molluscs and cnidarians, and followed by Kabeya et al. [40]. Alongside previously characterised Δ5 desaturases from molluscs and echinoderms, group A includes annelid sequences from each of the representative species from Clitellata and Polychaeta used in our analyses, with each species having one sole type A front-end desaturase (Fig. 2). Similarly, all assessed annelid species possessed at least one front-end desaturase candidate clustering in group B, which included previously characterised sequences from other invertebrates such as the mollusc *Sinonovacula constricta*. Additionally, a clade including the vertebrate front-end desaturases Fads1 and Fads2, and another one including front-end desaturases from echinoderms (group C), were also identified (Fig. 2). The putative front-end desaturases from *P. dumerilii*, *S. lamarcki*, *E. fetida*, *U. unicinctus* and *L. satsuma*, functionally characterised in the present study (see below), are highlighted in bold in Fig. 2. Sequences were deposited in the GenBank database under the accession numbers OQ102603 (PDfed1), OQ102604 (PDfed2), OQ102605 (PDfed3), OQ102606 (SLfed), OQ102608 (EFfed1), OQ102609 (EFfed2), OQ102610 (EFfed3), OQ102611 (UUfed) and OQ102612 (LSfed).

3.2. Roles of annelid front-end desaturases in LC-PUFA biosynthesis

In order to investigate the functional diversification of annelid front-end desaturases, a set of front-end desaturases selected according to the phylogenetic analysis results were expressed in yeast to ascertain their substrate specificities (Fig. 3). For the so-called group A, one sequence from the polychaetes *P. dumerilii* (PDfed1, acc. no. OQ102603) and *S. lamarcki* (SLfed, acc. no. OQ102606), and one from the clitellate *E. fetida* (EFfed1, acc. no. OQ102608) were investigated. The results showed that these front-end desaturases from group A were able to convert the PUFA substrates 20:3n-6 and 20:4n-3, into 20:4n-6 and 20:5n-3, respectively, suggesting that these enzymes are Δ5 desaturases (Table 2). Moreover, transgenic yeast expressing each of the three group A front-end desaturases assayed were able to introduce a Δ5 unsaturation into 20:2n-6 (20:2 $^{\Delta 11,14}$) and 20:3n-3 (20:3 $^{\Delta 11,14,17}$) to produce the non-methylene interrupted fatty acids (NMI-FA) 20:3 $^{\Delta 5,11,14}$ and 20:4 $^{\Delta 5,11,14,17}$, respectively (Table 2). No activity as Δ4, Δ6 or Δ8 was detected for any of the group A desaturases functionally characterised in the present study (Table 2). Additionally, the monoene 18:1n-13, resulting from the Δ5 desaturation towards the yeast endogenous 18:0 was systematically detected in all GC chromatograms from yeast expressing all the group A front-end desaturases (PDfed1, EFfed1 and SLfed).

For group B, sequences from the polychaetes *P. dumerilii* (PDfed2, acc. no. OQ102604; PDfed3, acc. no. OQ102605), *L. satsuma* (LSfed, acc. no. OQ102612) and *U. unicinctus* (UUfed, acc. no. OQ102611), and the

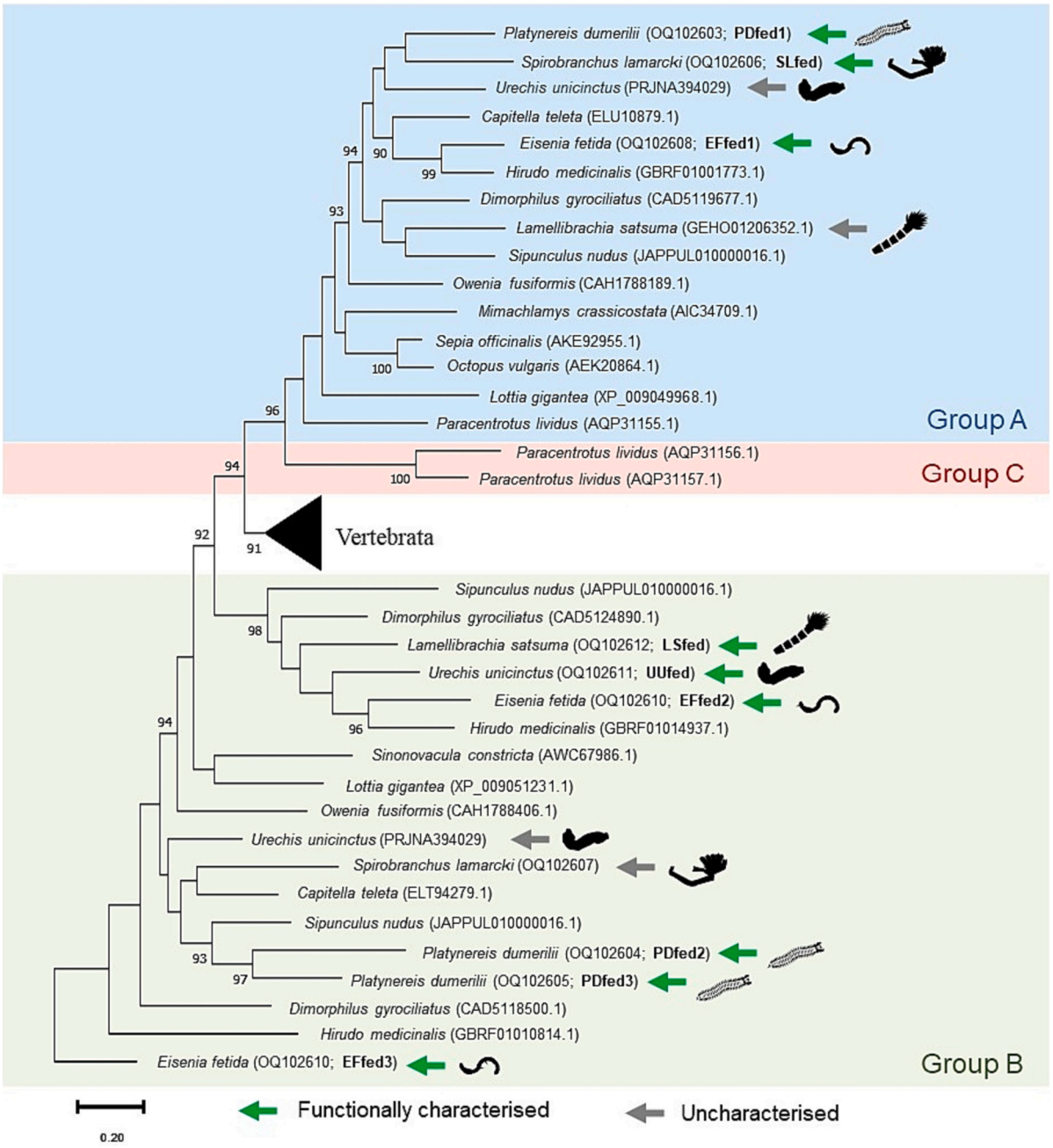

Fig. 2. Phylogenetic tree comparing the annelid front-end desaturase enzymes characterised in the present study with front-end desaturases from other animals. This is a resulting subtree representing the invertebrate front-end desaturases, the complete original tree can be found in Fig. S2. The transfer distance bootstrap support value (%) is given in each node when equal to or above 90 %.

clitellate *E. fetida* (EFfed2, acc. no. OQ102609; EFfed3, acc. no. OQ102610), were selected for functional analysis in yeast. As shown in Table 3, yeast expressing the PDfed2, LSfed and UUfed were able to convert the Δ6 desaturase substrates 18:2n-6 and 18:3n-3 into 18:3n-6 and 18:4n-3, respectively, as well as the Δ8 desaturase substrates 20:2n-6 and 20:3n-3 to 20:3n-6 and 20:4n-3, respectively. These results demonstrated that the group B PDfed2, LSfed and UUfed are dual Δ6 and Δ8 desaturases. Similar substrate specificities were also confirmed for the *E. fetida* EFfed2, although no desaturase product from 20:3n-3 was detected (Table 3). To clarify whether the apparent lack of Δ8 desaturation capacity by the *E. fetida* EFfed2 towards 20:3n-3 was compensated for by the other candidate sequence from group B existing in *E. fetida* (EFfed3), we also ran the functional assay for this putative desaturase. Our results showed that EFfed3 has Δ8 desaturation capacity, not only towards 20:2n-6 but also towards 20:3n-3, being converted to 20:3n-6 and 20:4n-3, respectively (Table 3). Interestingly, the *P. dumerilii* PDfed3, another representative of group B front-end desaturases, did not show any detectable activity towards any of the Δ6, Δ8, Δ5 and Δ4 substrates. Furthermore, to assess the capacity of group B desaturases to contribute to the DHA synthesis via the Sprecher Pathway (Fig. 1), transgenic yeast expressing the Δ6 front-end desaturase from *U. unicinctus* (UUfed) were grown in the presence of 24:5n-3. No desaturation products were identified (data not shown) confirming that its Δ6 desaturase activity is restricted to C_{18} PUFA substrates but does not recognise C_{24} as substrates.

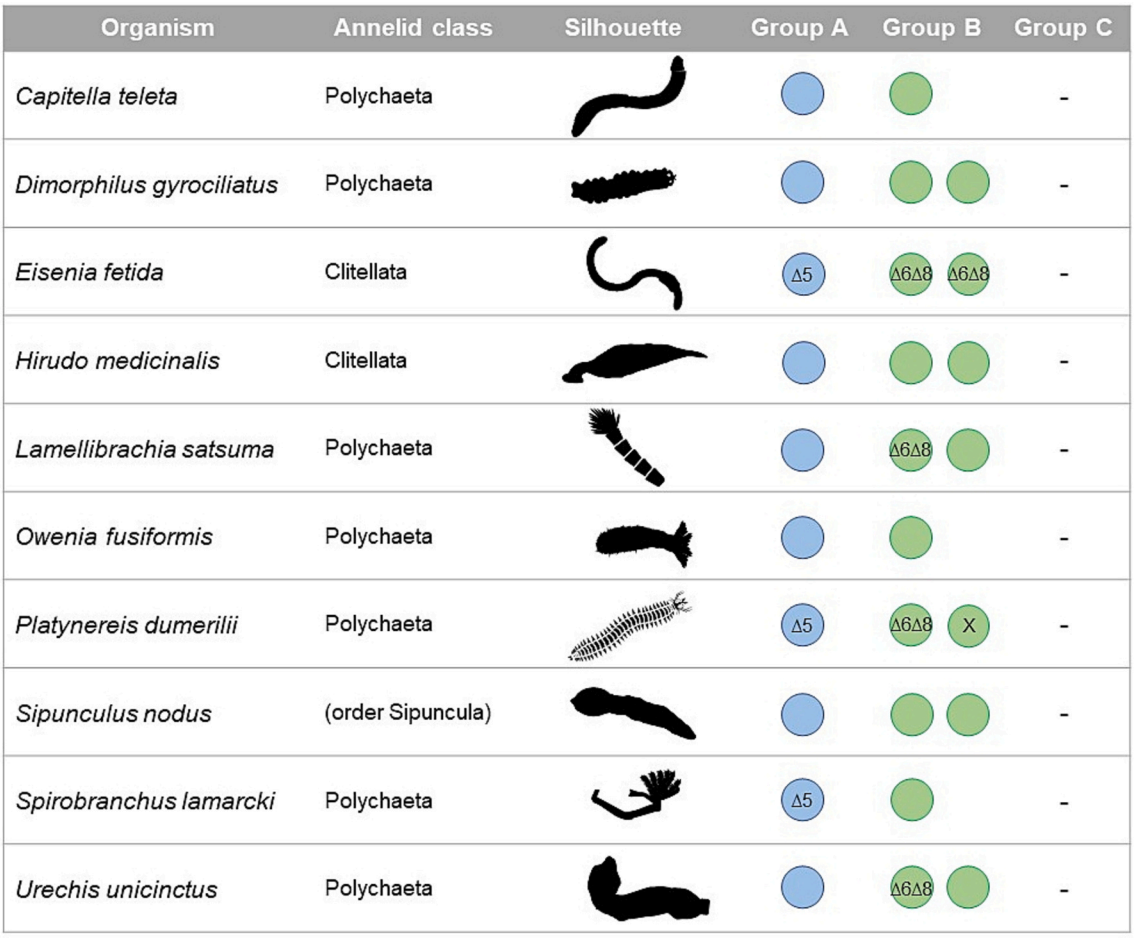

Fig. 3. Scheme of the front-end desaturase repertoire found in the annelids studied in this work. The blue circles represent the number of enzymes identified in group A, while the green circles represent the number of enzymes in group B. No front-end desaturases of group C were identified in annelids. The functional activity characterised in vitro of the enzymes tested in this work is shown inside the respective circle. If no activity was detected on the supplemented substrates in the enzyme assay, the circle is marked with an X inside.

Table 2
Functional characterisation of the group A front-end desaturases from *P. dumerilii* (PDfed1; OQ102603), *E. fetida* (EFfed1; OQ102608) and *S. lamarcki* (SLfed; OQ102606) in yeast. Conversions of supplemented PUFA substrates (18:2n-6, 18:3n-3, 20:2n-6, 20:3n-3, 20:3n-6, 20:4n-3, 22:4n-6, 22:5n-3) were calculated according to the formula [product area / (product area + substrate area) x 100]. *Non-methylene-interrupted fatty acids including 20:3 $^{\Delta5,11,14}$ and 20:4 $^{\Delta5,11,14,17}$ were detected as products of the enzymatic activity over 20:2n-6 (20:2 $^{\Delta11,14}$) and 20:3n-3 (20:3 $^{\Delta11,14,17}$), respectively.

Substrate	Product	PDfed1	EFfed1	SLfed	Activity
18:2n-6	18:3n-6	n.d.	n.d.	n.d.	Δ6
18:3n-3	18:4n-3	n.d.	n.d.	n.d.	Δ6
20:2n-6*	20:3n-6	n.d.	n.d.	n.d.	Δ8
20:3n-3*	20:4n-3	n.d.	n.d.	n.d.	Δ8
20:3n-6	20:4n-6	28.8	13.9	4.4	Δ5
20:4n-3	20:5n-3	39.6	18.5	1.0	Δ5
22:4n-6	22:5n-6	n.d.	n.d.	n.d.	Δ4
22:5n-3	22:6n-3	n.d.	n.d.	n.d.	Δ4

n.d., not detected.

4. Discussion

The present study aimed to investigate the gene complement and functional diversity of front-end desaturases in the phylum Annelida. A common feature shared among annelid front-end desaturases is the presence of a glutamine (Q) as the first aa within the third conserved H box [QXXHH] [27], which has previously been identified as a diagnostic residue of front-end desaturases in vertebrates [22,56] and other invertebrates [21,40,52,57,58]. Unlike front-end desaturases, other fatty acyl desaturases with major roles in LC-PUFA biosynthesis like methyl-end desaturases have a characteristic histidine (H) in the first position of the third H box, as seen in a variety of invertebrates, including polychaete annelids [11,15,16]. Moreover, while the second H box from front-end desaturases was suggested to typically contain three aa ("XXX") between the first and second H [HXXXHH] by Hashimoto et al. [27], front-end desaturases from annelids, as well as from other animals including both vertebrates [22,56] and invertebrates [21,40,57], have front-end desaturases with two aa residues ("XX") [HXXHH]. These results suggest that the H box composition along front-end desaturase sequences is more diverse than originally reported [27].

The phylogenetic analysis of the annelid front-end desaturases grouped them into two clusters termed group A and group B [54,55]. As expected, none of the annelid front-end desaturases clustered within the so-called group C, hypothesised to include only front-end desaturases from echinoderms [40]. As summarised in Fig. 3, we found that all representative species of the different annelid lineages possess a single front-end desaturase from group A. Interestingly, while all the species considered in the present study had at least one type B front-end desaturase, the number of front-end desaturases from group B varied among species, with a single sequence found in *S. lamarcki* and *L. satsuma*, and two distinct sequences existing in *E. fetida*, *P. dumerilii* and *U. unicinctus* (Fig. 3). Gene duplication of front-end desaturases was previously

Table 3
Functional characterisation of the group B front-end desaturases from *P. dumerilii* (PDfed2; OQ102604), *E. fetida* (EFfed2; OQ102609) (EFfed3; OQ102610), *L. satsuma* (LSfed; OQ102612) and *U. unicinctus* (UUfed; OQ102611) in yeast. Conversions of supplemented PUFA substrates (18:2n-6, 18:3n-3, 20:2n-6, 20:3n-3, 20:3n-6, 20:4n-3, 22:4n-6, 22:5n-3) were calculated according to the formula [product area / (product area + substrate area) × 100].

Substrate	Product	PDfed2	LSfed	UUfed	EFfed2	EFfed3	Activity
18:2n-6	18:3n-6	6.5	1.3	15.6	0.5	n.d.	Δ6
18:3n-3	18:4n-3	5.0	2.7	38.7	1.0	n.d.	Δ6
20:2n-6	20:3n-6	11.0	6.9	37.2	0.7	5.8	Δ8
20:3n-3	20:4n-3	22.9	19.1	64.3	n.d.	1.1	Δ8
20:3n-6	20:4n-6	n.d.	n.d.	n.d.	n.d.	n.d.	Δ5
20:4n-3	20:5n-3	n.d.	n.d.	n.d.	n.d.	n.d.	Δ5
22:4n-6	22:5n-6	n.d.	n.d.	n.d.	n.d.	n.d.	Δ4
22:5n-3	22:6n-3	n.d.	n.d.	n.d.	n.d.	n.d.	Δ4

n.d., not detected.

described in other invertebrates like molluscs [54], although restricted to specific classes such as gastropods and bivalves but not cephalopods, the latter having exclusively group A front-end desaturases [21,57].

Functional characterisation assays demonstrated that annelids possess front-end desaturases that, in combination, encompass Δ5, Δ6 and Δ8 activities in the enzyme set existing in a single species. Importantly, the number of enzymes involved in enabling such diverse desaturation capacity varies among species. All the annelid front-end desaturases from group A characterised in the present study showed Δ5 activity towards the PUFA substrates 20:3n-6 and 20:4n-3, which were desaturated into ARA (20:4n-6) and EPA (20:5n-3), respectively (Fig. 1). These results, along with their widespread distribution as shown here, support that Δ5 front-end desaturases play important roles is the provision of Δ5 desaturation products such as ARA and EPA that are naturally abundant in lipids from terrestrial annelids [59,60] like the herein investigated *E. fetida* [61], as well as aquatic species [17,18] including *Alitta virens*, a nereid polychaete like the herein studied *P. dumerilii* [19]. This is consistent with the occurrence of Δ5 front-end desaturases in other invertebrates like molluscs [21,57,62,63] and echinoderms [40], excluding the assessed Δ6 activity reported in the sea cucumber *A. japonicus* [64]. Indeed, the annelid Δ5 front-end desaturases characterised herein share further substrate specificities from those described in molluscs and echinoderms, including the capacity to biosynthesise 18:1n-13 and NMI-FA [21,40,57,62]. Clearly, all the annelid Δ5 front-end desaturases characterised in this study showed a peak identified as 18:1n-13 as a result of the activity of the assayed enzyme on the yeast endogenous 18:0. Occurrence of 18:1n-13 has been reported in sponges [65] and molluscs [66] but, to the best of our knowledge, no report of this monoene in annelids exists in the literature. However, several species of annelids have often been shown to have elongation products of 18:1n-13, including 20:1n-13, 20:2n-13 and 22:2n-13 [67,68], suggesting that biosynthesis of 18:1n-13 via Δ5 desaturation of 18:0 can occur.

In common with other invertebrates, the annelid Δ5 front-end desaturases can play a role in the biosynthesis of NMI-FA, as confirmed by the identification of $20{:}3^{\Delta5,11,14}$ and $20{:}4^{\Delta5,11,14,17}$ in transgenic yeast supplemented with $20{:}2^{\Delta11,14}$ and $20{:}3^{\Delta11,14,17}$, respectively. Similar results were previously found in group A front-end desaturases from the molluscs *Mimachlamys crassicostata* (former *Chlamys nobilis*; [62]), *S. constricta* [63], *O. vulgaris* [21] and *Sepia officinalis* [57], and the echinoderm *P. lividus* [40]. The importance and biological roles of NMI-FA in marine invertebrates remain unknown, although they are common components in lipids from sponges, molluscs, echinoderms and annelids [69]. In the case of polychaetes, NMI-FA were found at up to 12 % of the FA content in multiple deep-sea annelids species living in hydrothermal vents [67,70,71]. However, Makhutova et al. [60] did not detect the presence of NMI-FA in lipids from the aquatic clitellates *Lumbriculus variegatus* and *Tubifex tubifex*, even though these authors identified NMI-FA in the bivalves *Dreissena polymorpha* and *D. bugensis*. Similarly, NMI-FA were not reported in the FA profiles of the terrestrial clitellate *E. fetida* from several experiments [59,61,72]. Collectively, our results suggest that the origin of NMI-FA found, at least in polychaetes, is partly explained by endogenous production in which Δ5 front-end desaturases can play important roles.

Like group A front-end desaturases, annelid group B front-end desaturases have a widespread distribution across the phylum. However, rather than Δ5 desaturases, group B front-end desaturases from annelids have dual Δ6 and Δ8 desaturase capacities. Front-end desaturases with dual Δ6 and Δ8 desaturase capacities are commonly found in vertebrates including mammals [73] and teleosts [74], but had not been previously reported in other invertebrates like molluscs or echinoderms [13,50]. Instead, group B front-end desaturases have either Δ6 activity as reported for the razor clam *S. constricta* [63] or Δ8 activity such as in the noble scallop *M. crassicostata* [75] and the purple sea urchin *P. lividus* [40]. An exception to the general pattern of dual Δ6 and Δ8 activities in the group B front-end desaturases from annelids is illustrated by the type B front-end desaturase from *E. fetida*, which showed Δ8 activity but not Δ6. It is unclear whether the functional diversification of group B front-end desaturases observed in *E. fetida* is due to an adaptation to a naturally LC-PUFA deprived diet in terrestrial ecosystems. More generally, our results highlight the high functional diversification of front-end desaturases across the animal kingdom [13]. Importantly, further studies are required to clarify whether the herein characterised front-end desaturases can only operate towards acyl-CoA substrates as our yeast assays seem to imply or, alternatively, can also recognise phospholipid-linked substrates as reported for the Δ4 front-end desaturase from *Thraustochytrium* sp. [76].

Collectively, the results on gene complement and function of annelid front-end desaturases from the present study clearly show that these invertebrates have all the key desaturation activities required to bioconvert the two C_{18} PUFA precursors LA and ALA into the physiologically important LC-PUFA ARA and EPA, respectively, following two distinct routes, namely Δ6 desaturation – elongation – Δ5 desaturation, and elongation – Δ8 desaturation - Δ5 desaturation (Fig. 1). Our yeast-based assays do not allow us to identify which of the two pathways is more prominent, particularly in the absence of functional data on the PUFA elongase capacity. However, early studies suggested that some marine polychaetes such as *Arenicola marina* [18] and *A. virens* [19] have the "elongation – Δ8 desaturation – Δ5 desaturation" as the preferred route. Irrespective of which specific route enabling ARA and EPA biosynthesis is more prominent, our findings on the existence of active enzymatic networks for ARA and EPA biosynthesis strongly suggest that the characteristic high levels of ARA and EPA typically found in lipids from annelids can be accounted for by endogenous production involving the front-end desaturases reported here [17,18,59–61,68,77–80]. Nevertheless, it is important to note that the origin of some FA found in annelid lipids cannot be explained via biosynthesis. This appears to be the case of DHA, a LC-PUFA that can only be found at high levels in the lipids from annelids that have been fed on fish feed formulated with marine ingredients (fishmeal and fish oil) or with DHA-enriching diets (e.g., [61,68,78–80]). Consistent with this, lipids from annelids collected from wild populations have more moderate levels of DHA

[17,18,59–61,68,77–79]. Our dataset does not support a biosynthetic origin for DHA in the absence of front-end desaturases with, for example, Δ4 activity enabling direct synthesis of DHA from 22:5n-3 as occurs in some copepods (Fig. 1) [58,81]. Instead of the Δ4 pathway, the Sprecher pathway is an alternative route for DHA biosynthesis in vertebrates [82–85], but this pathway appears not to be active in annelids judging from the inability of the *U. unicinctus* Δ6 desaturase to bioconvert 24:5n-3 to 24:6n-3, which is the rate-limiting reaction within the Sprecher pathway (Fig. 1). While we cannot completely rule out the existence of annelid Δ6 front-end desaturases capable of producing 24:6n-3 from 24:5n-3, it is reasonable to speculate that a large proportion of the DHA found in lipids from the above studies on annelids has a dietary origin through retention/accumulation.

In conclusion, annelids possess at least two front-end desaturases that can perform Δ5 and Δ6Δ8 unsaturation reactions, enabling all the desaturation reactions required to bioconvert the C_{18} PUFA precursors into the biologically important LC-PUFA ARA and EPA. Such a gene repertoire is conserved across the different taxonomic groups existing within the phylum. Moreover, lack of front-end desaturases with Δ4 activity, and the apparent absence of activity producing 24:5n-3 by annelid Δ6 desaturation, strongly suggest that these invertebrates have limited capacity for DHA biosynthesis, with alternative lipid metabolic mechanisms accounting for the abundance of DHA often reported in the literature.

CRediT authorship contribution statement

Marc Ramos-Llorens: Investigation, Methodology, Formal analysis, Writing – original draft, Visualization. **Francisco Hontoria:** Conceptualization, Supervision, Writing – review & editing, Funding acquisition. **Juan C. Navarro:** Conceptualization, Methodology, Investigation, Supervision, Writing – review & editing, Funding acquisition. **David E.K. Ferrier:** Conceptualization, Supervision, Resources, Writing – review & editing. **Óscar Monroig:** Conceptualization, Supervision, Writing – review & editing, Funding acquisition.

Declaration of competing interest

The authors declare the following financial interests/personal relationships which may be considered as potential competing interests: Oscar Monroig reports financial support was provided by Agencia Estatal de Investigación. Juan C. Navarro reports financial support was provided by Generalitat Valenciana.

Data availability

Data will be made available on request.

Acknowledgements

The authors would like to thank Prof. Dr. Florian Raible for providing PIN inbreed strain *P. dumerilii*. This study was funded through the project IMPROMEGA Agencia Estatal de Investigación, Spain, grant no. RTI2018-095119-B-100, MCIN/AEI/FEDER/UE/MCIN/AEI/10.13039/501100011033/ and FEDER "A way to make Europe". Additionally, this study forms part of the ThinkInAzul programme and was supported by MCIN with funding from European Union NextGenerationEU (PRTR-C17.I1) and by Generalitat Valenciana (THINKINAZUL/2021/26).

Appendix A. Supplementary data

Supplementary data to this article can be found online at https://doi.org/10.1016/j.bbalip.2023.159377.

References

[1] J.P. Bergé, G. Barnathan, Fatty acids from lipids of marine organisms: molecular biodiversity, roles as biomarkers, biologically active compounds, and economical aspects, in: R. Ulber, Y. Le Gal (Eds.), Marine Biotechnology I, Advances in Biochemical Engineering/Biotechnology, 49-125, Springer, Berlin, Heidelberg, 2005, p. 96, https://doi.org/10.1007/b135782.
[2] M.I. Gladyshev, N.N. Sushchik, O.N. Makhutova, Production of EPA and DHA in aquatic ecosystems and their transfer to the land, Prostaglandins Other Lipid Mediat. 107 (2013) 117–126, https://doi.org/10.1016/j.prostaglandins.2013.03.002.
[3] S.M. Hixson, B. Sharma, M.j. Kainz, A. Wacker, M.T. Arts, Production, distribution, and abundance of long-chain omega-3 polyunsaturated fatty acids: a fundamental dichotomy between freshwater and terrestrial ecosystems, Environ. Rev. 23 (2015) 414–424, https://doi.org/10.1139/er-2015-0029.
[4] D. Swanson, R. Block, S.A. Mousa, Omega-3 fatty acids EPA and DHA: health benefits throughout life, Adv. Nutr. 3 (2012) 1–7, https://doi.org/10.3945/an.111.000893.
[5] J.H. Wu, R. Micha, F. Imamura, A. Pan, M.L. Biggs, O. Ajaz, L. Djousse, F.B. Hu, D. Mozaffarian, Omega-3 fatty acids and incident type 2 diabetes: a systematic review and meta-analysis, Br. J. Nutr. 107 (2012) S214–S227, https://doi.org/10.1017/S0007114512001602.
[6] J.E. Manson, N.R. Cook, I.M. Lee, W. Christen, S.S. Bassuk, S. Mora, H. Gibson, C. M. Albert, D. Gordon, T. Copeland, D. D'Agostino, G. Friedenberg, C. Ridge, V. Bubes, E.L. Giovannucci, W.C. Willett, J.E. Buring, Marine n-3 fatty acids and prevention of cardiovascular disease and cancer, N. Engl. J. Med. 380 (2019) 23–32, https://doi.org/10.1056/NEJMoa1811403.
[7] M.B. Schulze, A.M. Minihane, R.N.M. Saleh, U. Risérus, Intake and metabolism of omega-3 and omega-6 polyunsaturated fatty acids: nutritional implications for cardiometabolic diseases, Lancet Diabetes Endocrinol. 8 (2020) 915–930, https://doi.org/10.1016/S2213-8587(20)30148-0.
[8] S.M. Budge, E. Devred, M.H. Forget, V. Stuart, M.K. Trzcinski, S. Sathyendranath, T. Platt, Estimating concentrations of essential omega-3 fatty acids in the ocean: supply and demand, ICES J. Mar. Sci. 71 (2014) 1885–1893, https://doi.org/10.1093/icesjms/fsu003.
[9] H.C. Holm, H.F. Fredricks, S.M. Bent, D.P. Lowenstein, J.E. Ossolinski, K. W. Becker, W.M. Johnson, K. Schrage, B.A. Van Mooy, Global ocean lipidomes show a universal relationship between temperature and lipid unsaturation, Science 376 (2022) 1487–1491, https://doi.org/10.1126/science.abn74.
[10] S.L. Pereira, A.E. Leonard, P. Mukerji, Recent advances in the study of fatty acid desaturases from animals and lower eukaryotes, Prostaglandins Leukot. Essent. Fat. Acids 68 (2003) 97–106, https://doi.org/10.1016/S0952-3278(02)00259-4.
[11] N. Kabeya, M.M. Fonseca, D.E.K. Ferrier, J.C. Navarro, L.K. Bay, D.S. Francis, D. R. Tocher, L.F.C. Castro, Ó. Monroig, Genes for de novo biosynthesis of omega-3 polyunsaturated fatty acids are widespread in animals, Sci. Adv. 4 (2018), https://doi.org/10.1126/sciadv.aar6849.
[12] C.W. Twining, J.R. Bernhardt, A.M. Derry, C.M. Hudson, A. Ishikawa, N. Kabeya, M.J. Kainz, J. Kitano, C. Kowarik, S.N. Ladd, M.C. Leal, K. Scharnweber, J. R. Shipley, B. Matthews, The evolutionary ecology of fatty-acid variation: implications for consumer adaptation and diversification, Ecol. Lett. 24 (2021) 1709–1731, https://doi.org/10.1111/ele.13771.
[13] Ó. Monroig, A.C. Shu-Chien, N. Kabeya, D.R. Tocher, L.F.C. Castro, Desaturases and elongases involved in long-chain polyunsaturated fatty acid biosynthesis in aquatic animals: from genes to functions, Prog. Lipid Res. 86 (2022), 101157, https://doi.org/10.1016/j.plipres.2022.101157.
[14] A. Jakobsson, R. Westerberg, A. Jacobsson, Fatty acid elongases in mammals: their regulation and roles in metabolism, Prog. Lipid Res. 45 (2006) 237–249, https://doi.org/10.1016/j.plipres.2006.01.004.
[15] H. Liu, H. Wang, S. Cai, H. Zhang, A novel ω3-desaturase in the deep sea giant tubeworm *Riftia pachyptila*, Mar. Biotechnol. 19 (2017) 345–350, https://doi.org/10.1007/s10126-017-9753-9.
[16] N. Kabeya, I. Gür, A. Oboh, J.O. Evjemo, A.M. Malzahn, F. Hontoria, J.C. Navarro, Ó. Monroig, Unique fatty acid desaturase capacities uncovered in *Hediste diversicolor* illustrate the roles of aquatic invertebrates in trophic upgrading, Philos. Trans. R. Soc. B 375 (2020), 20190654, https://doi.org/10.1098/rstb.2019.0654.
[17] D.W. Pond, C.E. Allen, M.V. Bell, C.L. Van Dover, A.E. Fallick, D.R. Dixon, J. R. Sargent, Origins of long-chain polyunsaturated fatty acids in the hydrothermal vent worms *Ridgea piscesae* and *Protis hydrothermica*, Mar. Ecol. Prog. Ser. 225 (2002) 219–226, https://doi.org/10.3354/meps225219.
[18] P.J.W. Olive, T. Duangchinda, E. Ashforth, S. Craig, A.C. Ward, S.J. Davies, Net gain of long-chain polyunsaturated fatty acids (PUFA) in a lugworm *Arenicola marina* bioturbated mesocosm, Mar. Ecol. Prog. Ser. 387 (2009) 223–239, https://doi.org/10.3354/meps08088.
[19] S. Pairohakul, P.J.W. Olive, M.G. Bentley, G.S. Caldwell, Trophic upgrading of long-chain polyunsaturated fatty acids by polychaetes: a stable isotope approach using *Alitta virens*, Mar. Biol. 168 (2021) 67, https://doi.org/10.1007/s00227-021-03874-3.
[20] A. Weigert, C. Bleidorn, Current status of annelid phylogeny, Org. Divers. Evol. 16 (2016) 345–362, https://doi.org/10.1007/s13127-016-0265-7.
[21] Ó. Monroig, J.C. Navarro, J.R. Dick, F. Alemany, D.R. Tocher, Identification of a Δ5-like fatty acyl desaturase from the cephalopod *Octopus vulgaris* (Cuvier 1797) involved in the biosynthesis of essential fatty acids, Mar. Biotechnol. 14 (2012) 411–422, https://doi.org/10.1007/s10126-011-9423-2.
[22] N. Hastings, M. Agaba, D.R. Tocher, M.J. Leaver, J.R. Dick, J.R. Sargent, A.J. Teale, A vertebrate fatty acid desaturase with Delta 5 and Delta 6 activities, Proc. Natl.

Acad. Sci. U. S. A. 98 (2001) 14304–14309, https://doi.org/10.1073/pnas.251516598.
[23] J. Mistry, A. Bateman, R.D. Finn, Predicting active site residue annotations in the Pfam database, BMC Bioinform. 8 (2007) 298, https://doi.org/10.1186/1471-2105-8-298.
[24] J. Mistry, S. Chuguransky, L. Williams, M. Qureshi, G.A. Salazar, E.L. L. Sonnhammer, S.C.E. Tosatto, L. Paladin, S. Raj, L.J. Richardson, R.D. Finn, A. Bateman, Pfam: the protein families database in 2021, Nucleic Acids Res. 49 (2021) D412–D419, https://doi.org/10.1093/nar/gkaa913.
[25] P. Jones, D. Binns, H.Y. Chang, M. Fraser, W. Li, C. McAnulla, H. McWilliam, J. Maslen, A. Mitchell, G. Nuka, S. Pesseat, A.F. Quinn, A. Sangrador-Vegas, M. Scheremetjew, S.Y. Yong, R. Lopez, S. Hunter, InterProScan 5: genome-scale protein function classification, Bioinformatics 30 (2014) 1236–1240, https://doi.org/10.1093/bioinformatics/btu031.
[26] M. Blum, H.Y. Chang, S. Chuguransky, T. Grego, S. Kandasaamy, A. Mitchell, G. Nuka, T. Paysan-Lafosse, M. Qureshi, S. Raj, L. Richardson, G.S. Salazar, L. Williams, P. Bork, A. Bridge, J. Gough, D.H. Haft, I. Letunic, A. Marchler-Bauer, H. Mi, D.A. Natale, M. Necci, C.A. Orengo, A.P. Pandurangan, C. Rivoire, C.J. A. Sigrist, I. Sillitoe, N. Thanki, P.D. Thomas, S.C.E. Tosatto, C.H. Wu, A. Bateman, R.D. Finn, The InterPro protein families and domains database: 20 years on, Nucleic Acids Res. 49 (2021) D344–D354, https://doi.org/10.1093/nar/gkaa977.
[27] K. Hashimoto, A.C. Yoshizawa, S. Okuda, K. Kuma, S. Goto, M. Kanehisa, The repertoire of desaturases and elongases reveals fatty acid variations in 56 eukaryotic genomes, J. Lipid Res. 49 (2008) 183–191, https://doi.org/10.1194/jlr.M700377-JLR200.
[28] R.C. Edgar, MUSCLE: multiple sequence alignment with high accuracy and high throughput, Nucleic Acids Res. 32 (2004) 1792–1797, https://doi.org/10.1093/nar/gkh340.
[29] F. Lemoine, D. Correia, V. Lefort, O. Doppelt-Azeroual, F. Mareuil, S. Cohen-Boulakia, O. Gascuel, NGPhylogeny. fr: new generation phylogenetic services for non-specialists, Nucleic Acids Res. 47 (2019) W260–W265, https://doi.org/10.1093/nar/gkz303.
[30] O. Simakov, F. Marletaz, S.J. Cho, E. Edsinger-Gonzales, P. Havlak, U. Hellsten, D. H. Kuo, T. Larsson, J. Lv, D. Arendt, R. Savage, K. Osoegawa, P. de Jong, J. Grimwood, J.A. Chapman, H. Shapiro, A. Aerts, R.P. Otillar, A.Y. Terry, J. L. Boore, I.V. Grigoriev, D.R. Lindberg, E.C. Seaver, D.A. Weisblat, N.H. Putnam, D. S. Rokhsar, Insights into bilaterian evolution from three spiralian genomes, Nature 493 (2013) 526–531, https://doi.org/10.1038/nature11696.
[31] D. Hibsh, H. Schori, S. Efroni, O. Shefi, De novo transcriptome assembly databases for the central nervous system of the medicinal leech, Sci. Data 2 (2015), https://doi.org/10.1038/sdata.2015.15.
[32] A.K. Patra, Y.M. Kwon, Y. Fujiwara, S.G. Kang, S.J. Kim, De novo assembly and characterisation of *Lamellibrachia satsuma* transcriptome using HiSeq 2000 pair end sequencing, NCBI, 2017. https://www.ncbi.nlm.nih.gov/bioproject/PRJNA231974.
[33] T.B. Barton-Owen, R. Szabó, I.M.L. Somorjai, D.E.K. Ferrier, A revised spiralian homeobox gene classification incorporating new polychaete transcriptomes reveals a diverse TALE class and a divergent hox gene, Genome Biol. Evol. 10 (2018) 2151–2167, https://doi.org/10.1093/gbe/evy144.
[34] C. Park, Y.H. Han, S.G. Lee, K.B. Ry, J. Oh, E.M.A. Kern, J.K. Park, S.J. Cho, The developmental transcriptome atlas of the spoon worm *Urechis unicinctus* (Echiurida: Annelida), GigaScience 7 (2018) 1–7, https://doi.org/10.1093/gigascience/giy007.
[35] S. Schenk, S.C. Bannister, F.J. Sedlazeck, D. Anrather, B.Q. Minh, A. Bileck, M. Hartl, A. von Haeseler, C. Gerner, F. Raible, K. Tessmar-Raible, Combined transcriptome and proteome profiling reveals specific molecular brain signatures for sex, maturation and circalunar clock phase, Elife 8 (2019), e41556, https://doi.org/10.7554/eLife.41556.
[36] J.M. Martín-Durán, B.C. Vellutini, F. Marlétaz, V. Cetrangolo, N. Cvetesic, D. Thiel, S. Henriet, X. Grau-Bové, A.M. Carrillo-Baltodano, W. Gu, A. Kerbl, Y. Marquez, N. Bekkouche, D. Chourrout, J.L. Gómez-Skarmeta, M. Irimia, B. Lenhard, K. Worsaae, A. Hejnol, Conservative route to genome compaction in a miniature annelid, Nat. Ecol. Evol. 5 (2021) 231–242, https://doi.org/10.1038/s41559-020-01327-6.
[37] S. Short, A. Robinson, E. Lahive, A.G. Etxabe, S. Hernadi, M.G. Pereira, P. Kille, D. J. Spurgeon, Off-target stoichiometric binding identified from toxicogenomics explains why some species are more sensitive than others to a widely used neonicotinoid, Environ. Sci. Technol. 55 (2021) 3059–3069, https://doi.org/10.1021/acs.est.0c05125.
[38] F.M. Martín-Zamora, Y. Liang, K. Guynes, A.M. Carrillo-Baltodano, B.E. Davies, R. D. Donnellan, Y. Tan, G. Moggioli, O. Seudre, M. Tran, K. Mortimer, N. M. Luscombe, A. Hejnol, F. Marlétaz, J.M. Martín-Durán, Annelid functional genomics reveal the origins of bilaterian life cycles, Nature 615 (2023) 105–110, https://doi.org/10.1038/s41586-022-05636-7.
[39] Y. Qi, L. Chen, B. Wu, X. Tang, X. Zhu, R. Li, K. Wu, H. Luo, *Sipunculus nudus* genome provides insights into evolution of spiralian phyla and development, Front. Mar. Sci. 9 (2023), 1043311, https://doi.org/10.3389/fmars.2022.1043311.
[40] N. Kabeya, A. Sanz-Jorquera, S. Carboni, A. Davie, A. Oboh, Ó. Monroig, Biosynthesis of polyunsaturated fatty acids in sea urchins: molecular and functional characterisation of three fatty acyl desaturases from *Paracentrotus lividus* (Lamark 1816), PLoS One 12 (2017), e0169374, https://doi.org/10.1371/journal.pone.0169374.
[41] K. Katoh, D.M. Standley, MAFFT multiple sequence alignment software version 7: improvements in performance and usability, Mol. Biol. Evol. 30 (2013) 772–780, https://doi.org/10.1093/molbev/mst010.
[42] S. Capella-Gutiérrez, J.M. Silla-Martínez, T. Gabaldón, trimAl: a tool for automated alignment trimming in large-scale phylogenetic analyses, Bioinformatics 25 (2009) 1972–1973, https://doi.org/10.1093/bioinformatics/btp348.
[43] S. Guindon, J.F. Dufayard, V. Lefort, M. Anisimova, W. Hordijk, O. Gascuel, New algorithms and methods to estimate maximum-likelihood phylogenies: assessing the performance of PhyML 3.0, Syst. Biol. 59 (2010) 307–321, https://doi.org/10.1093/sysbio/syq010.
[44] V. Lefort, J.E. Longueville, O. Gascuel, SMS: smart model selection in PhyML, Mol. Biol. Evol. 34 (2017) 2422–2424, https://doi.org/10.1093/molbev/msx149.
[45] F. Lemoine, J.B. Domelevo Entfellner, E. Wilkinson, D. Correia, M. Dávila Felipe, T. De Oliveira, O. Gascuel, 2018. Renewing Felsenstein's phylogenetic bootstrap in the era of big data, Nature 556 (2018) 452–456, https://doi.org/10.1038/s41586-018-0043-0.
[46] T. Junier, E.M. Zdobnov, The Newick utilities: high-throughput phylogenetic tree processing in the UNIX shell, Bioinformatics 26 (2010) 1669–1670, https://doi.org/10.1093/bioinformatics/btq243.
[47] K. Tamura, G. Stecher, S. Kumar, MEGA11: molecular evolutionary genetics analysis version 11, Mol. Biol. Evol. 38 (2021) 3022–3027, https://doi.org/10.1093/molbev/msab120.
[48] J. Zantke, S. Bannister, V.B. Veedin Rajan, F. Raible, K. Tessmar-Raible, Genetic and genomic tools for the marine annelid *Platynereis dumerilii*, Genetics 197 (2014) 19–31, https://doi.org/10.1534/genetics.112.148254.
[49] O. Folmer, M. Black, W. Hoeh, R. Lutz, R. Vrijenhoek, DNA primers for amplification of mitochondrial cytochrome c oxidase subunit I from diverse metazoan invertebrates, Mol. Mar. Biol. Biotechnol. 3 (1994) 294–299.
[50] Ó. Monroig, N. Kabeya, Desaturases and elongases involved in polyunsaturated fatty acid biosynthesis in aquatic invertebrates: a comprehensive review, Fish. Sci. 84 (2018) 911–928, https://doi.org/10.1007/s12562-018-1254-x.
[51] J. Folch, M. Lees, G.H. Sloane Stanley, A simple method for the isolation and purification of total lipides from animal tissues, J. Biol. Chem. 226 (1957) 497–509, https://doi.org/10.1016/S0021-9258(18)64849-5.
[52] A. Ribes-Navarro, J.C. Navarro, F. Hontoria, N. Kabeya, I.B. Standal, J.O. Evjemo, Ó. Monroig, Biosynthesis of long-chain polyunsaturated fatty acids in marine gammarids: molecular cloning and functional characterisation of three fatty acyl elongases, Mar. Drugs 19 (2021) 226, https://doi.org/10.3390/MD19040226.
[53] W.W. Christie, A simple procedure for rapid transmethylation of glycerolipids and cholesteryl esters, J. Lipid Res. 23 (1982) 1072–1075, https://doi.org/10.1016/S0022-2275(20)38081-0.
[54] J.M. Surm, P.J. Prentis, A. Pavasovic, Comparative analysis and distribution of omega-3 lcPUFA biosynthesis genes in marine molluscs, PLoS One 10 (2015), e0136301, https://doi.org/10.1371/journal.pone.013630.
[55] J.M. Surm, T.M. Toledo, P.J. Prentis, A. Pavasovic, Insights into the phylogenetic and molecular evolutionary histories of Fad and Elovl gene families in Actiniaria, Ecol. Evol. 8 (2018) 5323–5335, https://doi.org/10.1002/ece3.4044.
[56] A. Marquardt, H. Stöhr, K. White, B.H. Weber, cDNA cloning, genomic structure, and chromosomal localization of three members of the human fatty acid desaturase family, Genomics 66 (2000) 175–183, https://doi.org/10.1006/geno.2000.6196.
[57] Ó. Monroig, F. Hontoria, I. Varó, D.R. Tocher, J.C. Navarro, Investigating the essential fatty acids in the common cuttlefish *Sepia officinalis* (Mollusca, Cephalopoda): molecular cloning and functional characterisation of fatty acyl desaturase and elongase, Aquaculture 450 (2016) 38–47, https://doi.org/10.1016/j.aquaculture.2015.07.003.
[58] J. Boyen, A. Ribes-Navarro, N. Kabeya, Ó. Monroig, A. Rigaux, P. Fink, P. I. Hablützel, J.C. Navarro, M. De Troch, Functional characterisation reveals a diverse array of metazoan fatty acid biosynthesis genes, Mol. Ecol. 32 (2022) 970–982, https://doi.org/10.1111/mec.16808.
[59] R.P. Hansen, Z. Czochanska, The fatty acid composition of the lipids of earthworms, J. Sci. Food Agric. 26 (1975) 961–971, https://doi.org/10.1002/jsfa.2740260713.
[60] O.N. Makhutova, N.N. Sushchik, M.I. Gladyshev, A.V. Ageev, E.G. Pryanichnikova, G.S. Kalachova, Is the fatty acid composition of freshwater zoobenthic invertebrates controlled by phylogenetic or trophic factors? Lipids 46 (2011) 709–721, https://doi.org/10.1007/s11745-011-3566-9.
[61] M. Kumlu, A. Beksari, O.T. Eroldoğan, H.A. Yılmaz, M. Sarıipek, E. Kınay, G. M. Turchini, DHA enrichment of the red earthworm *Eisenia fetida* for improving its potential as dietary source for aquaculture, Aquaculture 496 (2018) 10–18, https://doi.org/10.1016/j.aquaculture.2018.07.005.
[62] H. Liu, Z. Guo, H. Zheng, S. Wang, Y. Wang, W. Liu, G. Zhang, Functional characterization of a Δ5-like fatty acyl desaturase and its expression during early embryogenesis in the noble scallop *Chlamys nobilis* Reeve, Mol. Biol. Rep. 41 (2014) 7437–7445, https://doi.org/10.1007/s11033-014-3633-4.
[63] Z. Ran, J. Xu, K. Liao, S. Li, S. Chen, X. Yan, Biosynthesis of polyunsaturated fatty acids in the razor clam *Sinonovacula constricta*: characterisation of Δ5 and Δ6 fatty acid desaturases, J. Agric. Food Chem. 66 (2018) 4592–4601, https://doi.org/10.1021/acs.jafc.8b00968.
[64] X. Liu, L. Wang, Z. Feng, X. Song, W. Zhu, Molecular cloning and functional characterization of the fatty acid delta 6 desaturase (FAD6) gene in the sea cucumber *Apostichopus japonicus*, Aquac. Res. 48 (2017) 4991–5003, https://doi.org/10.1111/are.13317.
[65] J.D. Joseph, Lipid composition of marine and estuarine invertebrates: Porifera and Cnidaria, Prog. Lipid Res. 18 (1979) 1–30, https://doi.org/10.1016/0163-7827(79)90002-X.
[66] J.D. Joseph, Lipid composition of marine and estuarine invertebrates. Part II: Mollusca, Prog. Lipid Res. 21 (1982) 109–153, https://doi.org/10.1016/0163-7827(82)90002-9.

[67] V.I. Kharlamenko, A.S. Maiorova, E.V. Ermolenko, Fatty acid composition as an indicator of the trophic position of abyssal megabenthic deposit feeders in the Kuril Basin of the Sea of Okhotsk, Deep-Sea Res. II Top. Stud. Oceanogr. 154 (2018) 374–382, https://doi.org/10.1016/j.dsr2.2018.03.005.
[68] D. Jerónimo, A.I. Lillebø, E. Maciel, M.R.M. Domingues, J. Cremades, R. Calado, Unravelling the fatty acid profiles of different polychaete species cultured under integrated multi-trophic aquaculture (IMTA), Sci. Rep. 11 (2021) 10812, https://doi.org/10.1038/s41598-021-90185-8.
[69] G. Barnathan, Non-methylene-interrupted fatty acids from marine invertebrates: occurrence, characterisation and biological properties, Biochimie 91 (2009) 671–678, https://doi.org/10.1016/j.biochi.2009.03.020.
[70] C.F. Phleger, M.M. Nelson, A.K. Groce, S.C. Cary, K.J. Coyne, P.D. Nichols, Lipid composition of deep-sea hydrothermal vent tubeworm *Riftia pachyptila*, crabs *Munidopsis subsquamosa* and *Bythograea thermydron*, mussels *Bathymodiolus sp*. and limpets *Lepetodrilus spp*, Comp. Biochem. Physiol. B: Biochem. Mol. Biol. 141 (2005) 196–210, https://doi.org/10.1016/j.cbpc.2005.03.001.
[71] C.F. Phleger, M.M. Nelson, A.K. Groce, S.C. Cary, K. Coyne, J.A. Gibson, P. D. Nichols, Lipid biomarkers of deep-sea hydrothermal vent polychaetes—*Alvinella pompejana*, *A. caudata*, *Paralvinella grasslei* and *Hesiolyra bergii*, Deep-Sea Res. I Oceanogr. Res. Pap. 52 (2005) 2333–2352, https://doi.org/10.1016/j.dsr.2005.08.001.
[72] B. Gunya, P.J. Masika, A. Hugo, V. Muchenje, Nutrient composition and fatty acid profiles of oven-dried and freeze-dried earthworm *Eisenia foetida*, J. Food Nutr. Res. 4 (2016) 343–348, https://doi.org/10.12691/jfnr-4-6-1.
[73] W.J. Park, K.S. Kothapalli, P. Lawrence, C. Tyburczy, J.T. Brenna, An alternate pathway to long-chain polyunsaturates: the FADS2 gene product Delta8-desaturates 20:2n-6 and 20:3n-3, J. Lipid Res. 50 (2009) 1195–1202, https://doi.org/10.1194/jlr.M800630-JLR200.
[74] O. Monroig, Y. Li, D.R. Tocher, Delta-8 desaturation activity varies among fatty acyl desaturases of teleost fish: high activity in delta-6 desaturases of marine species, Comp. Biochem. Physiol. B Biochem. Mol. Biol. 159 (2011) 206–213, https://doi.org/10.1016/j.cbpb.2011.04.007.
[75] H. Liu, H. Zhang, H. Zheng, S. Wang, Z. Guo, G. Zhang, PUFA biosynthesis pathway in marine scallop *Chlamys nobilis* reeve, J. Agric. Food Chem. 62 (2014) 12384–12391, https://doi.org/10.1021/jf504648f.
[76] J.L. Yilmaz, Z.L. Lim, M. Beganovic, S. Breazeale, C. Andre, S. Stymne, P. Vrinten, T. Senger, Determination of substrate preferences for desaturases and elongases for production of docosahexaenoic acid from oleic acid in engineered canola, Lipids 52 (2017) 207–222, https://doi.org/10.1007/s11745-017-4235-4.
[77] J. García-Alonso, C.T. Müller, J.D. Hardege, Influence of food regimes and seasonality on fatty acid composition in the ragworm, Aquat. Biol. 4 (2008) 7–13, https://doi.org/10.3354/ab00090.
[78] A.A. Bischoff, P. Fink, U. Waller, The fatty acid composition of *Nereis diversicolor* cultured in an integrated recirculated system: possible implications for aquaculture, Aquaculture 296 (2009) 271–276, https://doi.org/10.1016/j.aquaculture.2009.09.002.
[79] F. Salvo, S.C. Dufour, D. Hamoutene, C.C. Parrish, Lipid classes and fatty acids in *Ophryotrocha cyclops*, a dorvilleid from Newfoundland aquaculture sites, PLoS One 10 (2015), e0136772, https://doi.org/10.1371/journal.pone.0136772.
[80] B. Marques, A.I. Lillebø, F. Ricardo, C. Nunes, M.A. Coimbra, R. Calado, Adding value to ragworms (*Hediste diversicolor*) through the bioremediation of a super-intensive marine fish farm, Aquac. Environ. Interact. 10 (2018) 79–88, https://doi.org/10.3354/aei00255.
[81] N. Kabeya, M. Ogino, H. Ushio, Y. Haga, S. Satoh, J.C. Navarro, Ó. Monroig, A complete enzymatic capacity for biosynthesis of docosahexaenoic acid (DHA, 22:6n-3) exists in the marine harpacticoida copepod *Tigriopus californicus*, Open Biol. 11 (2021), 200402, https://doi.org/10.1098/rsob.200402.
[82] H. Sprecher, Metabolism of highly unsaturated n-3 and n-6 fatty acids, Biochim. Biophys. Acta, Lipids Lipid Metab. 1486 (2000) 219–231, https://doi.org/10.1016/S1388-1981(00)00077-9.
[83] M. Buzzi, R.J. Henderson, J.R. Sargent, The desaturation and elongation of linolenic acid and eicosapentaenoic acid by hepatocytes and liver microsomes from rainbow trout (*Oncorhynchus mykiss*) fed diets containing fish oil or olive oil, Biochim. Biophys. Acta, Lipids Lipid Metab. 1299 (1996) 235–244, https://doi.org/10.1016/0005-2760(95)00211-1.
[84] M. Buzzi, R.J. Henderson, J.R. Sargent, Biosynthesis of docosahexaenoic acid in trout hepatocytes proceeds via 24-carbon intermediates, Comp. Biochem. Physiol. B: Biochem. Mol. Biol. 116 (1997) 263–267, https://doi.org/10.1016/s0305-0491(96)00210-6.
[85] A. Oboh, N. Kabeya, G. Carmona-Antoñanzas, L.F.C. Castro, J.R. Dick, D.R. Tocher, Ó. Monroig, Two alternative pathways for docosahexaenoic acid (DHA, 22:6n-3) biosynthesis are widespread among teleost fish, Sci. Rep. 7 (2017) 3889, https://doi.org/10.1038/s41598-017-04288-2.